

Analysis of chlorophyll *a* concentration along the Galician coast: seasonal variability and trends

I. Alvarez^{1,2}, M. N. Lorenzo^{1*}, and M. deCastro¹

¹EPPhysLab (Environmental Physics Laboratory), Facultad de Ciencias, Universidade de Vigo, Ourense, Spain

²CESAM, Departamento de Física, Universidade de Aveiro, Aveiro, Portugal

*Corresponding author: tel: +34 988 387329; fax: +34 988 387227; e-mail: nlorenzo@uvigo.es

Alvarez, I., Lorenzo, M. N., and deCastro, M. 2012. Analysis of chlorophyll *a* concentration along the Galician coast: seasonal variability and trends. – ICES Journal of Marine Science, 69: 728–738.

Received 4 May 2011; accepted 12 January 2012; advance access publication 5 April 2012.

The spatial and temporal distribution of chlorophyll *a* (Chl *a*) concentration was analysed along the Galician coast from 1998 to 2007. Sea surface temperature and Ekman transport data were also used to investigate the relationship between the ocean–atmosphere conditions and Chl *a* formation and variability. The west coast showed the highest Chl *a* concentration, with three peaks of maximum values (February, April–May, and July–September). Along the central coast, the pattern was similar, with the highest concentrations measured during spring and summer, but with lower values. The north coast was the least productive, with much lower values. The high seasonal variability of Chl *a* was mainly related to upwelling events during spring and summer. During autumn and winter, Chl *a* variations depended on other factors such as the input of nutrients from land run-off. There was no clear seasonal trend in Chl *a*.

Keywords: chlorophyll *a*, Ekman transport, Galician coast, sea surface temperature.

Introduction

Ocean chlorophyll *a* (Chl *a*) concentration can be highly sensitive to changes in sea surface temperature (SST) and windforcing. Several analyses of oceanic temperature around the world have revealed a global warming trend in the ocean (Levitus *et al.*, 2000), which can have a negative impact on marine ecosystems. This warming has also been observed at a regional scale over the Atlantic area (Gomez-Gesteira *et al.*, 2008; deCastro *et al.*, 2009). As a consequence of warming, latitudinal displacements of population (phytoplankton and zooplankton) have been reported in regions of the North Atlantic (Richardson and Schoeman, 2004; Richardson, 2008), with increasing phytoplankton abundance in cooler regions and decreasing phytoplankton abundance in warmer ones. Global warming can also intensify alongshore winds and accelerate coastal upwelling circulation (Bakun, 1990).

The Galician coast (NW Iberian Peninsula) is at the northernmost limit of the eastern North Atlantic upwelling system (Wooster *et al.*, 1976). Previous studies have shown that this region has a seasonal wind regime (for a detailed description of wind patterns along the Galician coast, see Torres *et al.*, 2003; Gomez-Gesteira *et al.*, 2006; Alvarez *et al.*, 2008b). Typically, during the dry season (April–September), the wind blows southwards along the coast, generating upwelling-favourable

conditions, and during the wet season (October–March), the wind is northwards (upwelling-unfavourable). Nevertheless, the mean long-term windfields are not necessarily representative of certain years when summer upwelling patterns also dominate in winter (Borges *et al.*, 2003; deCastro *et al.*, 2006, 2008). Over this region, therefore, coastal upwelling is mainly during spring and summer (Fraga, 1981; Botas *et al.*, 1990; Bode *et al.*, 2002; Llope *et al.*, 2006; Alvarez *et al.*, 2008a, 2010; Borja *et al.*, 2008; Fontan *et al.*, 2008), although it can also be observed in autumn and winter (Santos *et al.*, 2001; Borges *et al.*, 2003; deCastro *et al.*, 2006, 2008; Alvarez *et al.*, 2009).

Owing to the regularity of upwelling events, the area exhibits enhanced primary production because of the presence of nutrient-rich water masses that are upwelled towards surface layers. Several water masses have been identified around the Galician coast. From spring to summer, eastern North Atlantic central water (ENACW), a cold and nutrient-rich water mass from greater depth, is found near the coast (Fiuza, 1984; Rios *et al.*, 1992). During late autumn and winter, Galician offshore seawater is under the influence of the Iberian Poleward Current (IPC), a saline, warm, surface current whose occurrence and intensity varies between years (Frouin *et al.*, 1990; Haynes and Barton, 1990). Therefore, during spring and summer, upwelling events

cause the ENACW to reach the surface layers, generating the high primary production that supports the notable biological diversity in the region (Tenore *et al.*, 1995). Winter events can pump IPC water inside the estuaries along the coast (Prego *et al.*, 2007), increasing the salinity of estuarine waters and reducing their nutrient content.

In recent decades, several studies of the Chl *a* concentration have been carried out in the area, mainly during spring and summer (Casas *et al.*, 1997; Castro *et al.*, 2000; Bode *et al.*, 2002, 2009; Varela *et al.*, 2005; Otero *et al.*, 2008). Most of these studies focused on data measured at isolated stations located in different regions of the coast, providing localized knowledge of Chl *a* patterns in space. The development of satellite remote-sensing technology, however, allowed routine, high-resolution measurements of Chl *a* over the oceans. These observations can help to characterize the behaviour of primary production over vast areas by revealing the distribution of Chl *a*. Taking advantage of satellite data, the present study aims to investigate the seasonal variability in Chl *a* concentration along the Galician coast from 1998 to 2007.

The Galician coast can be subdivided into three domains (Figure 1): the west coast, south of Cape Finisterre; the central coast, from Cape Finisterre to Cape Ortegal; and the north coast, east of Cape Ortegal. Therefore, the spatial and temporal distribution of Chl *a* concentration is analysed in these three domains. Further, SST and Ekman transport data are used to characterize the ocean–atmosphere conditions that lead to the formation and variability of Chl *a* concentrations. In addition, recent

trends in Chl *a* concentration and SST are analysed based on monthly values.

The paper is organized as follows. In the “Data and methods” section, the different datasets and the methodologies used in the analysis are described. Then, spatial and temporal patterns of Chl *a* SST and Ekman transport are analysed before the relationships between Chl *a* and the ocean–atmospheric conditions are investigated. Finally, a summary and conclusions are presented.

Data and methods

The analysis of Chl *a* concentration along the Galician coast was based on data obtained from the Sea-viewing Wide Field-of-view Sensor (SeaWiFS). Data were obtained from NASA’s Goddard Space Flight Center (<http://oceancolor.gsfc.nasa.gov/SeaWiFS/>) for the period 1998–2007, with a spatial resolution of 9 km and a temporal resolution of 8 d. Three types of analysis were carried out with these data. First, the monthly average SeaWiFS Chl *a* concentrations were considered along the whole coastline under study for the period 1998–2007. Second, mean monthly concentrations were analysed at several control points located along the west, central, and north coasts (Figure 1, dots). Third, three polygons were considered over the shelf along the Galician coast covering coastal areas between the coast and the 200-m isobath (Figure 1, polygons I, II and III; thin black line). Chl *a* concentration inside each polygon was spatially averaged to obtain a mean value every 8 d.

To estimate SST variations, weekly mean SST data were obtained from night-time measurements carried out by the Advanced Very High Resolution Radiometer (AVHRR) on board NOAA series satellites (<http://poet.jpl.nasa.gov>) for the period 1998–2007, with a spatial resolution of 4 km. For each gridpoint, an SST value was computed as the average of all cloud-free multi-channel measurements available for 1 week. SST monthly averaged data were analysed along the whole Galician coast for the full study period, and in the three polygons shown in Figure 1 (thin black line), weekly data were analysed.

Surface windfields, available from July 1999, were obtained from the QuikSCAT satellite. Wind data were retrieved from the Jet Propulsion Laboratory website (http://podaac.jpl.nasa.gov/DATA_CATALOG/quikscatinfo.html) as a level 3 scientific product. The dataset consists of values of meridional and zonal components of wind estimated twice daily on an approximately $0.25 \times 0.25^\circ$ grid, with global coverage. An average of the two daily measurements was taken. Windspeed measurements range from 3 to 20 m s^{-1} (accuracy 2 m s^{-1} and 20° in direction). The reference height of wind data is 10 m. It is important to note that wind data close to the coast (25 km) are not available because of the existence of a small land mask. However, previous studies have shown that QuikSCAT data are comparable with modelled data in the area (Gómez-Gesteira *et al.*, 2006; Alvarez *et al.*, 2008b; Penabad *et al.*, 2008).

The Ekman transport can be calculated in terms of the windspeed from the QuikSCAT satellite, W , by

$$Q_x = \frac{\rho_a C_d}{\rho_w f} (W_x^2 + W_y^2)^{1/2} W_y \quad \text{and}$$

$$Q_y = -\frac{\rho_a C_d}{\rho_w f} (W_x^2 + W_y^2)^{1/2} W_x,$$

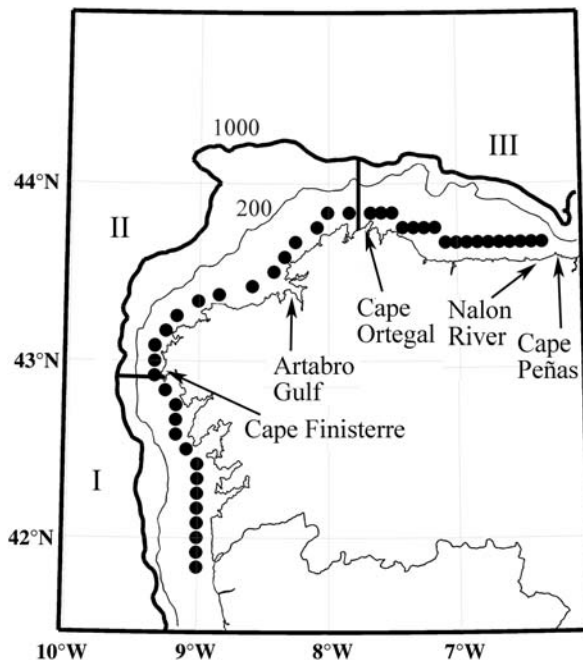


Figure 1. Map of the Galician coast. Polygons I, II, and III are the regions selected to analyse Chl *a*, SST, and Ekman transport values. The three regions cover the coastal areas between coast and the 200-m isobath (thin black line) for Chl *a* and SST and between the coast and the 1000-m isobath (heavy black line) for Ekman transport. Black points are where the mean monthly concentrations of Chl *a* were analysed.

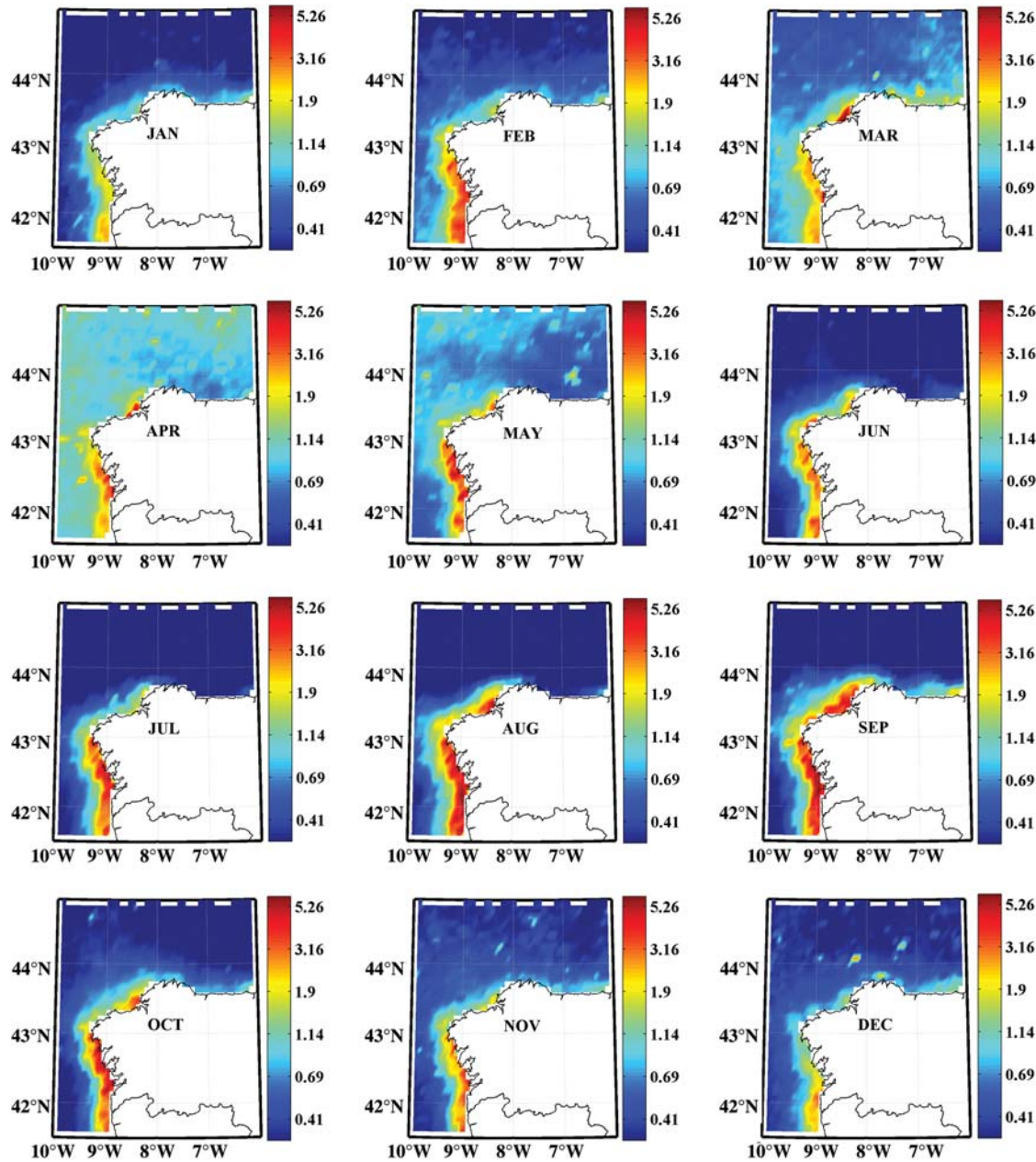


Figure 2. Monthly mean distributions of Chl *a* concentration (mg m^{-3}) from 1998 to 2007 along the Galician coast. Colour contouring corresponds to Chl *a* concentration on a logarithmic scale.

where air density $\rho_a = 1.22 \text{ kg m}^{-3}$, seawater density $\rho_w = 1025 \text{ kg m}^{-3}$, $C_d = 1.4 \times 10^{-3}$, a dimensionless drag coefficient, and f is the Coriolis parameter, defined as twice the vertical component of the Earth's angular velocity, Ω , about the local vertical given by $f = 2\Omega \sin(\theta)$ at latitude θ . The subscript x corresponds to the zonal component and the subscript y to the meridional one. Monthly averages of the Ekman transport were analysed along the whole Galician coast. In addition, as for Chl *a* and SST, the Ekman transport was spatially averaged inside the three polygons between the coast and the 1000-m isobath (Figure 1, thick black line). In this case, the polygons cover a large area with respect to the Chl *a* and SST data owing to the land mask present in the QuikSCAT data.

An upwelling index (UI) can be calculated as the Ekman transport component in the direction perpendicular to the shoreline

(Bakun, 1973; Nykjaer and Van Camp, 1994; Gomez-Gesteira *et al.*, 2006) from $UI = Q_\perp = -\sin(\theta)Q_x + \cos(\theta)Q_y$, where $\theta = \pi/2 + \phi$, and ϕ is the angle of the unitary vector perpendicular to the shoreline pointing landwards. Positive (negative) UI values mean upwelling-favourable (-unfavourable) conditions.

Spatio-temporal patterns of Chl *a*, SST, and Ekman transport

Variability in Chl *a* concentration

The concentrations of Chl *a* along the Galician coast, obtained from monthly averages of SeaWiFS data from 1998 to 2007, were generally higher in coastal areas, showing high seasonal variability (Figure 2). In winter (January–March), the maximum

values ($2\text{--}3 \text{ mg m}^{-3}$) were along the west coast, and along the central and north coasts, Chl *a* concentrations were lower ($0.5\text{--}1 \text{ mg m}^{-3}$).

These high values along the west coast are related to the input of nutrients from the land through river discharge (Miño River; Figure 1). In addition, winter upwelling events can also occur (Santos *et al.*, 2001; Borges *et al.*, 2003; deCastro *et al.*, 2006, 2008; Alvarez *et al.*, 2009), bringing nutrient-rich water from lower depths during that season. Some of the existing studies (deCastro *et al.*, 2008; Varela *et al.*, 2010) have demonstrated the presence of cold, nutrient-rich water near the coast that can be attributed to ENACW.

From April to September, Chl *a* concentrations increased south of Cape Finisterre ($4\text{--}5 \text{ mg m}^{-3}$) and were also noticeable along the central coast. In August and September, a continuous band of high values was observed from Cape Ortegal to the southern part of the west coast. The high concentrations during spring are in agreement with the known spring blooms that usually overlap with upwelling blooms from May to October. This situation can be related to the upwelling events being more frequent south of Cape Finisterre (Gómez-Gesteira *et al.*, 2006; Alvarez *et al.*, 2008b). Along the north coast, the Chl *a* concentrations decreased from spring to summer.

In autumn (October–December), maximum values of Chl *a* concentration were observed again along the west coast, although the values were lower ($2\text{--}3 \text{ mg m}^{-3}$) than in summer. In contrast, along the north coast, higher concentrations were observed than in summer.

The seasonal variability of Chl *a* concentration can be analysed spatially better by considering the west, central, and north coasts separately. The mean annual evolution of Chl *a* concentration measured at the control points (Figure 3) was considered for each coastal area (Figure 1, black points). Along the west coast (Figure 3a), there were three peaks of high concentration, the first in February with the maximum values ($2.5\text{--}3 \text{ mg m}^{-3}$) in front of the Galician Rias Baixas ($\sim 42.5^\circ\text{N}$) and in front of the Miño River mouth ($\sim 42^\circ\text{N}$), the second corresponded to spring months (April–May), with maximum values (3.5 mg m^{-3}) around the Galician Rias Baixas, and third during summer (July–September), when maximum values (4 mg m^{-3}) were seen over almost all the region. These results coincide with those of Bode *et al.* (2009) in a control station located off the western Galician coast using dataseries collected from 1989 to 2006. Those authors found that in recent years, blooms in summer increased relative to those in early spring or autumn, in contrast to the period 1991–1995.

At the control points along the central coast (Figure 3b), the situation was similar to that of the west coast. Concentrations were highest during spring and summer, but with lower values (1.5 and 3 mg m^{-3} , respectively) mainly in front of the Artabro Gulf.

Along the north coast (Figure 3c), the Chl *a* pattern was different, with the highest concentrations in early spring (March) and autumn (September–October), and the lowest ones in summer (June–August). In addition, values were much lower than along the west and central coasts (maximum 1.5 mg m^{-3}). This situation is characteristic of the typical planktonic cycle along the Cantabrian coast: winter mixing followed by summer stratification and phytoplankton blooms developing in the transition periods: mixing–stratification (spring bloom) and stratification–mixing (autumn bloom; Varela *et al.*, 2005, 2008, 2010). In December,

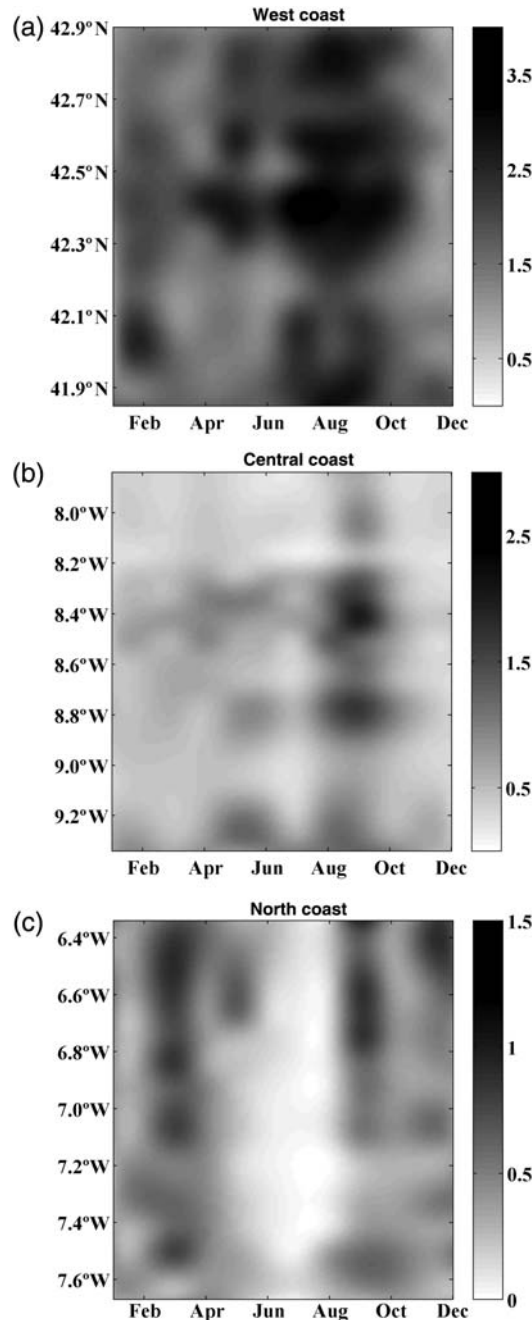


Figure 3. Mean annual evolution of Chl *a* (mg m^{-3}) from 1998 to 2007 calculated at the control points (Figure 1) situated along the (a) west, (b) central, and (c) north Galician coasts.

concentrations were high (1.2 mg m^{-3}) at the most easterly point, around Cape Peñas. These values were most probably attributable to the delivery of nutrients by the Nalon River discharge (Figure 1), the most important river in terms of freshwater flux and nutrient-loading into the area (Prego and Vergara, 1998).

In summary, the west coast is the most productive, followed by the central and north coasts. Along the west coast, Chl *a* peaks three times annually, the first time in February, the second in spring, and the third in summer. The monthly Miño River discharge (the most important river along this coast) averaged from 1998 to 2007 and the monthly UI data averaged from 2000

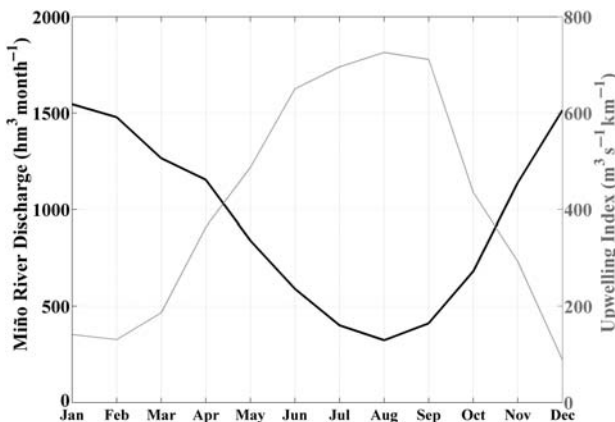


Figure 4. Monthly Miño River discharge averaged from 1998 to 2007 (black line) and the monthly *UI* ($\text{m}^3 \text{s}^{-1} \text{km}^{-1}$) averaged from 2000 to 2007 (thin dotted line) inside polygon I (Figure 1).

to 2007 (obtained from QuikSCAT data) inside polygon I (Figure 1, thick black line) provide additional insight into these patterns (Figure 4). River discharge (black line) showed a typical pattern, with high values during winter and low values in summer. These values ranged from $1500 \text{ hm}^3 \text{ month}^{-1}$ in February to $300 \text{ hm}^3 \text{ month}^{-1}$ in September. In contrast, the *UI* (grey line) was at its maximum in summer ($700 \text{ m}^3 \text{ s}^{-1} \text{ km}^{-1}$) and at its minimum in winter ($100 \text{ m}^3 \text{ s}^{-1} \text{ km}^{-1}$). Consequently, the most important forcing during winter was river discharge, whereas during summer it was *UI*. Therefore, the high Chl *a* concentration observed along the west coast during February (spring–summer) is likely fuelled by the river discharge (and upwelling events). Nevertheless, although the *UI* during winter is lower than during summer, the values are not negligible and can create winter upwelling events that deliver nutrient-rich water (deCastro et al., 2008; Varela et al., 2010) and generate an increased Chl *a* concentration. The absence of available river discharge data into the central and north coastal areas prevents a similar analysis. However, the occurrence of Chl *a* maximum during spring and summer indicates that the most important forcing may be the upwelling events.

Ekman transport patterns

To understand the formation and seasonal variability of Chl *a* concentration along the coast, the atmospheric conditions were analysed in terms of the Ekman transport. The monthly average of the Ekman transport along the Galician coast calculated from QuikSCAT winds shows variation between the different months (Figure 5). In winter (January–March), the maximum transport values ($350 \text{ m}^3 \text{ s}^{-1} \text{ km}^{-1}$) were along the west and north coasts, and the minimum ones along the central coast. Nevertheless, transport direction showed two different patterns. In January and March, the transport was mainly directed southwards all along the coast, whereas in February the transport was westwards south of Cape Finisterre and southwards north of that point.

These patterns agree with those found by Alvarez et al. (2008a) along the west coast of the Iberian Peninsula. Those authors analysed upwelling variability along the coast from 1967 to 2006 and found a strong seasonality characterized by upwelling-favourable conditions from April to September and unfavourable conditions

from October to March. Nevertheless, upwelling-favourable conditions were observed in February during the past decade (1997–2006). This result was corroborated by sea level pressure composites, which showed the existence of abnormally high pressures close to the Iberian Peninsula during that decade compared with the historical records (analysed from 1948).

Therefore, the February pattern showed upwelling-favourable conditions along the west coast that could generate winter upwelling events in the area. In fact, the results agree with several winter upwelling events described during the past decade (deCastro et al., 2006, 2008; Prego et al., 2007; Varela et al., 2010). These winter events can be related to the presence of ENACW or IPC water near the coast, which can be upwelled inside the estuaries located throughout the area. Increased quantities of IPC water result in greater salinity and reduced dissolved nutrients, whereas increased amounts of ENACW can result in greater productivity, although to a less extent than during a summer upwelling event (Prego et al., 2007). Most of the winter upwelling events studied along the western Galician coast up to now have been associated with the presence of ENACW near the coast (deCastro et al., 2008; Varela et al., 2010). Therefore, the peak of Chl *a* concentration observed in February along this coast (Figure 3a) may be explained, in addition to river discharge, by the upwelling events following favourable conditions indicated by the Ekman transport (Figure 5) and the presence of a nutrient-rich water mass (i.e. ENACW) which can be upwelled from the lower depths.

During spring and summer (April–September), Ekman transport values are highest along the west coast ($350 \text{ m}^3 \text{ s}^{-1} \text{ km}^{-1}$) and lowest along the north coast. The pattern is characterized by the existence of westward transport along the west and central coasts and southward transport along the northern one, showing that the most upwelling-favourable conditions are south of Cape Finisterre (Gómez-Gesteira et al., 2006; Alvarez et al., 2008b).

In September, although transport intensity was similar to that observed in earlier months, transport direction was slightly different. Transport along the north coast was seawards, producing upwelling-favourable conditions almost all along the coast. Atmospheric conditions during spring and summer agree with the Chl *a* patterns characterized above (Figures 2 and 3), with concentrations in spring and summer highest along the west and central coasts and lowest along the north coast. The occurrence of spring–summer upwelling events may explain this difference between coasts. These events are associated with the presence of ENACW near the west and central coasts (Fraga, 1981; Bode et al., 2002; Alvarez et al., 2005, 2008a) which fertilizes coastal waters and fuels primary production. ENACW was also present along the north coast, resulting in increased primary production (Fernandez and Bode, 1991; Llorente et al., 2006), although less notable than that observed south of Cape Finisterre (Varela et al., 2005).

From October to December, the transport pattern changes again. In October and December, transport was southwards all along the coast, with highest values along the north coast. In November, the pattern was similar to that observed in February, although with lower intensity (maximum $300 \text{ m}^3 \text{ s}^{-1} \text{ km}^{-1}$). South of Cape Finisterre transport is westwards, indicating upwelling-favourable conditions. However, the Chl *a* concentration (Figures 2 and 3) measured during November was lower than during February. These results indicate the need for further research in terms especially of winter upwelling events and their possible impact on biological productivity.

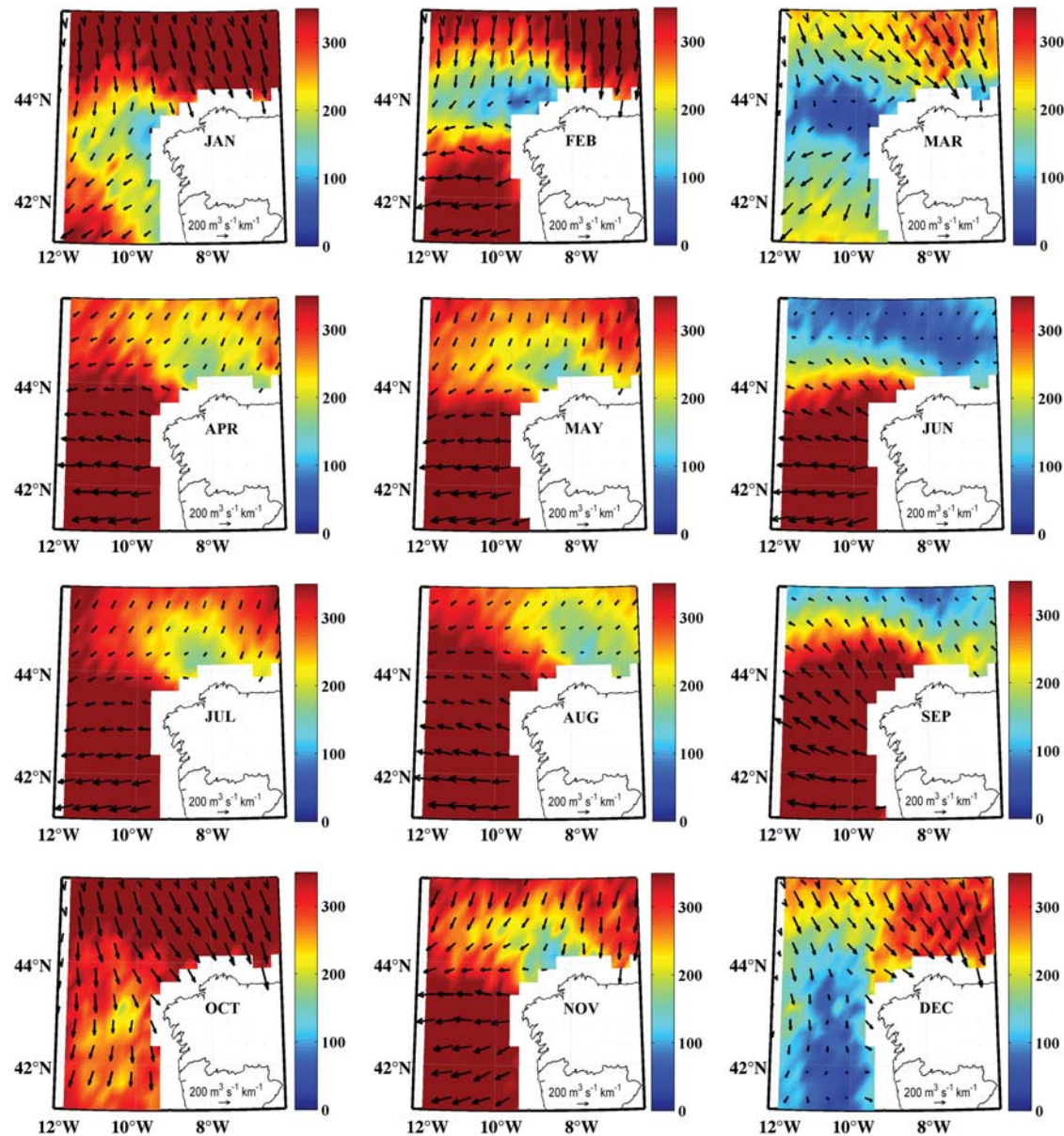


Figure 5. Monthly mean distributions of Ekman transport (arrows and colour contouring are $\text{m}^3 \text{s}^{-1} \text{km}^{-1}$) from 2000 to 2007 along the Galician coast.

Variability in SST

Monthly averages of SST were analysed to reveal the oceanic conditions (Figure 6). SST along the Galician coast was highly variable throughout the year. In winter (January–March), maximum temperature (14.5°C) was in the southern part of the west coast. In addition, in January, a filament of water warmer than the surrounding coastal and oceanic water was observed turning east at Cape Finisterre. This warm water corresponds to the IPC, which normally arrives in the Cantabrian Sea at the start of every winter (Ambar *et al.*, 1986; Frouin *et al.*, 1990; Garcia-Soto *et al.*, 2002; deCastro *et al.*, 2011). The band of colder water between the IPC water and the nearshore water of the west coast was attributable to water cooled as a result of net heat loss from the surface during the preceding months (Fiuza, 1983; desChamps *et al.*, 1984).

In February, it was also possible to see a band of colder water near the west coast, although less obviously than in January. In this case, the tongue of colder water may be explained by the presence of upwelled water resulting from upwelling-favourable conditions (Figure 5) supporting the high Chl *a* concentration observed then (Figures 2 and 3). In March, which marks the transition to spring, a tongue of warm water from the southern latitudes was observed along the west coast from nearshore to open-ocean latitudes. The same situation was observed in April and May.

From June to September, the maximum temperature was in the eastern part of the north coast. This pattern is due to the SST warming observed in spring–summer at the southeastern corner of the Bay of Biscay (Pingree and Le Cann, 1989; Koutsikopoulos and Le Cann, 1996; Gomez-Gesteira *et al.*, 2008). A band of colder water was present nearshore along the

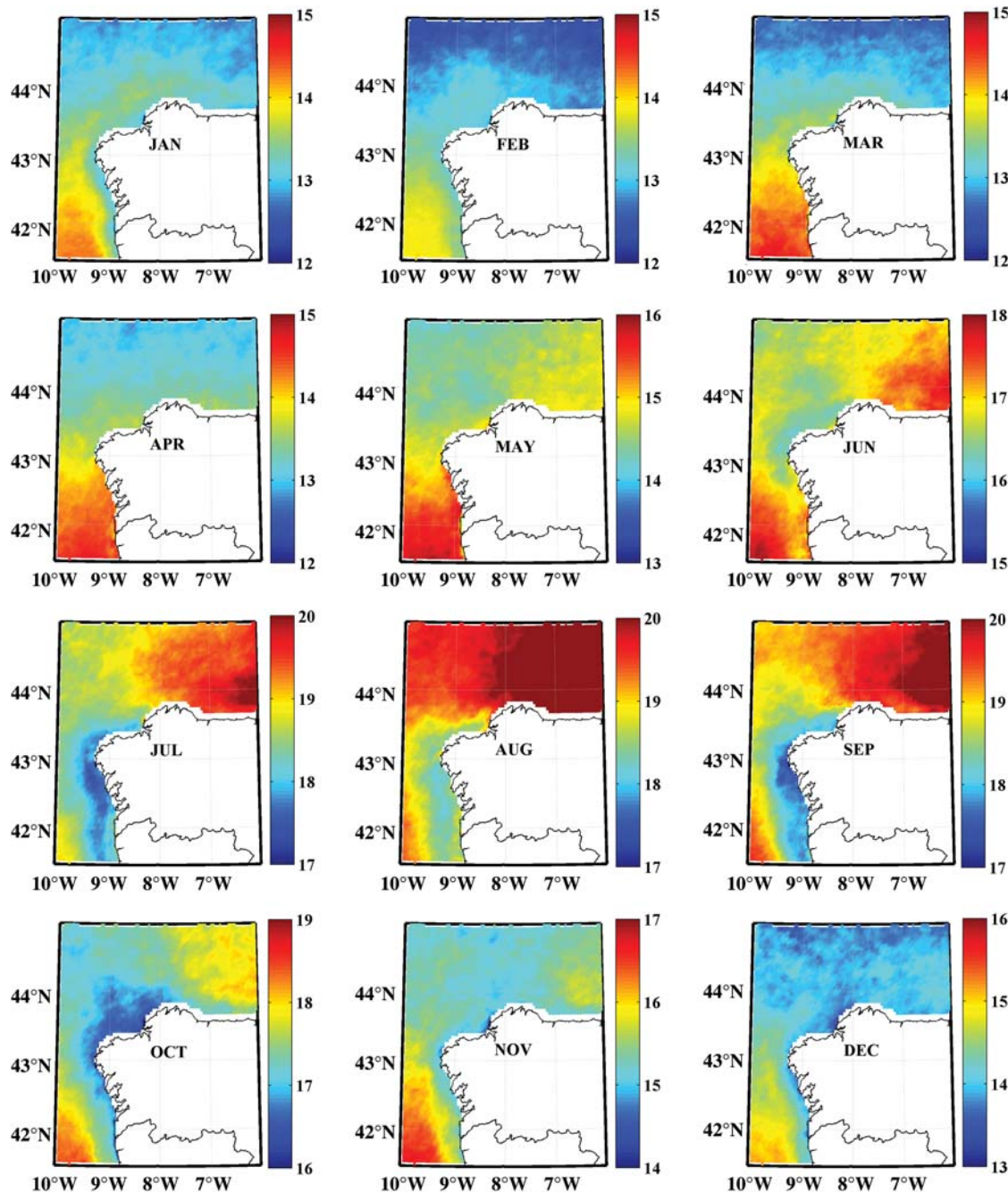


Figure 6. Monthly mean distributions of SST ($^{\circ}\text{C}$) from 1998 to 2007 along the Galician coast.

central and west coasts, generating a longitudinal gradient in SST. The appearance of this colder water was related to the intense north winds that produce upwelling-favourable conditions during those months (Figure 5). These events brought cold, nutrient-rich water from the lower depths, resulting in increased primary production (Figures 2 and 3) and the generation of the tongue of cold water.

October marks the transition to autumn in these latitudes, with the input of colder water from northern latitudes. Hence, temperature decreased from October to December along the north coast and SST values were highest (18°C) along the west coast. A band of colder water along the west coast was also present during

these months and may be attributable to winter upwelling events (Figure 3, November) or to water cooled as a result of net heat loss from the surface (Fiuza, 1983; desChamps *et al.*, 1984).

Relationship between coastal Chl α concentration and ocean–atmosphere conditions

Temporal evolution

The anomalies in Chl α concentration, SST, and UI were calculated for the west, central, and north coasts (Figure 7), taking into account the average monthly data inside the three polygons shown in Figure 1. Chl α and SST data were depicted from 1998

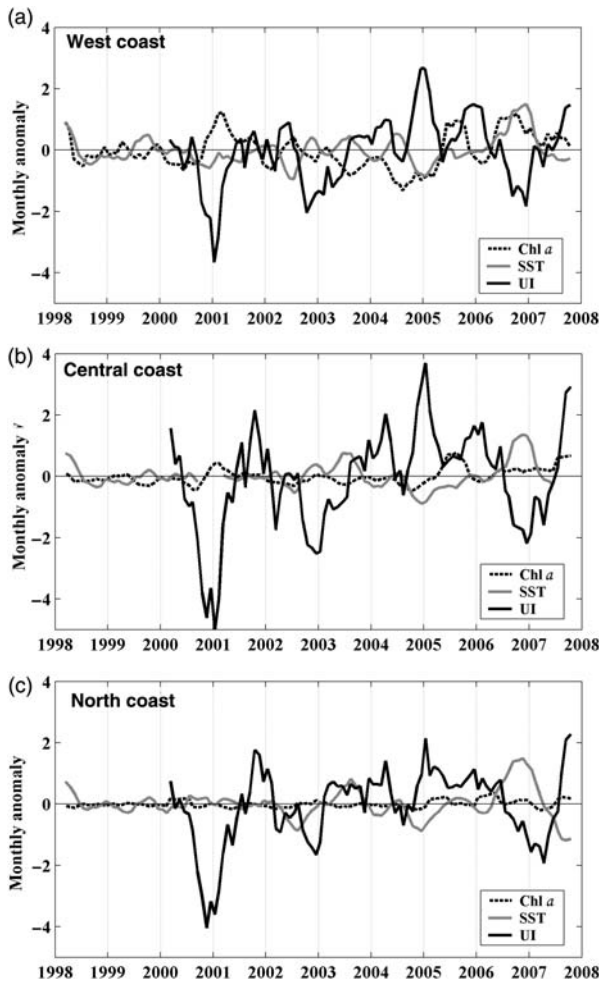


Figure 7. Monthly anomaly of Chl *a* (mg m^{-3} , black dashed line), SST ($^{\circ}\text{C}$, grey line), and UI ($\text{m}^3 \text{s}^{-1} \text{km}^{-1}$, black line) calculated at the (a) western, (b) central, and (c) northern Galician coast taking into account the average data inside the three polygons shown in Figure 1. The period analysed for Chl *a* and SST is 1998–2007 and for Ekman transport 2000–2007.

to 2007 and UI from 2000 to 2007. A 2-month running average was used to follow the overall trends in the time-series, although such a running average can remove some of the variation.

There were some differences among years for the three variables, as well as differences in the amplitudes of the signals over the period. Given the interannual evolution (Figure 7), it is difficult to analyse the response of coastal Chl *a* concentration to oceanic (SST) and atmospheric (wind) conditions. Based on the results obtained above, two seasons have been considered: dry (April–September) and wet (October–March). The analysis was carried out using the correlation coefficient for each season based on monthly values (Table 1), and it produced correlations between Chl *a* and UI anomalies and between Chl *a* and SST anomalies inside the three polygons (Figure 1).

From April to September, Chl *a* and UI were positively correlated right along the coast, with the maximum value in the central area (0.55) and the minimum along the north coast (0.22). During the same period, there was a negative correlation (around -0.30) between Chl *a* and SST. These correlations

Table 1. Correlations between Chl *a*, UI, and SST calculated considering the monthly anomaly values averaged inside the three polygons shown in Figure 1, with correlations between Chl *a* and UI corresponding to the period 2000–2007 and between Chl *a* and SST to the period 1998–2007.

| Coast | Chl <i>a</i> vs. UI | | Chl <i>a</i> vs. SST | |
|---------|---------------------|---------------|----------------------|---------------|
| | April–September | October–March | April–September | October–March |
| West | 0.38* | -0.65^* | -0.31^* | 0.42* |
| Central | 0.55* | -0.77^* | -0.33^* | 0.52* |
| North | 0.22 | -0.18 | – | 0.56* |

* $p < 0.05$.

indicate high Chl *a* associated with cold surface water generated by upwelling events that transport deep, cold, nutrient-rich waters to the surface. During autumn and winter, Chl *a* was negatively correlated with UI and positively correlated with SST, indicating that high/low Chl *a* values were related to warm/cold waters and to upwelling-unfavourable/favourable conditions. Whereas during spring and summer the Chl *a* variations can be explained mainly by the upwelling events, during autumn and winter this variability could depend to a greater extent on other factors, such as the input of nutrients from land run-off (Wang *et al.*, 2006). Hence, during the dry season, primary production was more often nutrient-limited, so was tightly coupled to the upwelling of nutrients, whereas during the wet season, primary production was more likely to be light-limited, so less tightly tied to the upwelling of nutrients.

An example of this situation can be seen in Figure 7a, where at the end of 2000 and the start of 2001, a notable negative anomaly of the UI was associated with a positive anomaly of Chl *a*. This period was characterized by intense southerly winds (upwelling-unfavourable conditions), which brought to the coast the Atlantic depressions and associated adverse weather conditions with high rainfall events (Alvarez *et al.*, 2005). The high rainfall resulted in discharges from the rivers along the coast that generated high concentrations of particulate organic matter, which are clear in the SeaWiFS data.

Spatial trends

Recent trends in Chl *a* concentration and SST have also been analysed taking into account the monthly anomaly values calculated from 1998 to 2007 in the three polygons shown in Figure 1. Trends in UI were not calculated because of the high annual variability in wind patterns (for a detailed description of trends in wind patterns over the region, see Alvarez *et al.*, 2008a, 2010, 2011). Instead, trends were calculated by fitting the monthly anomalies to a straight line, considering the dry season and the wet season separately. Only a few values show a significant trend ($p < 0.05$; Table 2).

Chl *a* showed a significant positive trend during spring–summer along the western and central coasts, with values between 0.6 and $1 \text{ mg m}^{-3} \text{ decade}^{-1}$. The north coast did not show such a clear trend. On the contrary, from October to March, there was a significant negative trend along the west coast (approximately $-0.5 \text{ mg m}^{-3} \text{ decade}^{-1}$) and a positive trend along the northern one ($\sim 0.2 \text{ mg m}^{-3} \text{ decade}^{-1}$).

Trends in SST were significant only during spring and summer along the west and north coasts, with values of $\sim 0.4^{\circ}\text{C decade}^{-1}$.

Table 2. Trends in Chl *a* and SST calculated using the monthly anomaly values averaged from 1998 to 2007 inside the three polygons shown in Figure 1.

| Coast | Chl <i>a</i> ($\text{mg m}^{-3} \text{ decade}^{-1}$) | | SST ($^{\circ}\text{C decade}^{-1}$) | |
|---------|---|---------------|--|---------------|
| | April–September | October–March | April–September | October–March |
| West | 1.01* | −0.53* | 0.44* | 0.32 |
| Central | 0.62* | −0.03 | 0.11 | 0.16 |
| North | − | 0.16* | 0.42* | −0.01 |

* $p < 0.05$.

These results agree with the seasonal SST trends calculated by Gomez-Gesteira *et al.* (2008) along the Atlantic Arc from 1985 to 2005. Those authors found a significant positive trend along the whole west coast of the Iberian Peninsula during spring and summer, with values of $\sim 0.3\text{--}0.4^{\circ}\text{C decade}^{-1}$. In contrast, along the Cantabrian coast, the only significant trend was in spring, with a value of $\sim 0.4^{\circ}\text{C decade}^{-1}$. SST and Chl *a* trends indicate that both variables tended to increase during spring and summer over the past decade (Table 2).

Overview of findings

The seasonal and interannual variability and the 10-year trend of chlorophyll along the Galician coasts were analysed from 1998 to 2007 taking into account the spatial and temporal distribution of Chl *a* concentration. SST data and the UI were used to analyse the forcing mechanisms that explained Chl *a* concentration and variability. The results obtained from this study have shown the main results listed below.

- Chl *a* concentration had a different annual cycle within each coastal area, with high seasonal variability. The west coast was the most productive coast of Galicia, with three peaks of maximum Chl *a*. The first was in February, the second between April and May, and the third from July to September. The central coast showed two peaks of high concentration corresponding to spring and summer, although with lower values. The north coast was the least productive. The highest Chl *a* concentrations were observed in early spring (March) and autumn (September and October), although with much lower values than those of the west and central coasts.
- The seasonality of Chl *a* was mainly related to the spring–summer upwelling events, which are more frequent along the central and west coasts. In spring and summer, Chl *a* concentration increased south of Cape Ortegal (Figure 1), primarily near the coast. This pattern is related to the existence of intense northerly winds along the continental shelf that cause upwelling of cold, nutrient-rich water to the upper layers, supporting high Chl *a* concentration. These upwelling-favourable conditions during spring and summer were also corroborated by the SST analysis, which revealed the presence of a tongue of cold water near the coast.
- Chl *a* concentration in autumn and winter could also be influenced by upwelling events mainly south of Cape Finisterre. In February and November, the Ekman transport was westwards along the west coast, providing upwelling-favourable conditions. These winter events can bring cold, nutrient-rich water

from the lower depths, resulting in an increase in Chl *a* concentration and generating the tongue of cold water.

- Coastal Chl *a* concentration did not obviously respond to oceanic and atmospheric conditions. From the correlation analysis, it was clear that during spring and summer, the Chl *a* variation can be explained mainly by the upwelling events, whereas during autumn and winter, the variability depends on factors such as the input of nutrients from land run-off.
- There was no clear seasonal trend in Chl *a* or SST. Chl *a* showed significant positive trends during spring and summer and negative trends during autumn and winter along the west and central coasts. The trend in SST was significantly positive only during spring and summer along the west and north coasts.

Acknowledgements

The work was supported by Xunta de Galicia under project 10PXIB383169PR and co-financed by the European Regional Development Fund (FEDER). IA is supported by the Ministerio de Ciencia e Innovacion through the Ramon y Cajal Program.

References

- Alvarez, I., deCastro, M., Gomez-Gesteira, M., and Prego, R. 2005. Inter- and intra- annual analysis of the salinity and temperature evolution in the Galician Rías Baixas–ocean boundary (northwest Spain). *Journal of Geophysical Research*, 110: C04008. doi:10.1029/2004JC002504.
- Alvarez, I., Gomez-Gesteira, M., deCastro, M., and Dias, J. M. 2008a. Spatio-temporal evolution of the upwelling regime along the western coast of the Iberian Peninsula. *Journal of Geophysical Research*, 113: C07020. doi:10.1029/2008JC004744.
- Alvarez, I., Gomez-Gesteira, M., deCastro, M., Gomez-Gesteira, J. L., and Dias, J. M. 2010. Summer upwelling frequency along the western Cantabrian coast from 1967 to 2008. *Journal of Marine Systems*, 79: 218–226.
- Alvarez, I., Gomez-Gesteira, M., deCastro, M., Lorenzo, M. N., Crespo, A. J. C., and Dias, J. M. 2011. Comparative analysis of upwelling influence between the western and northern coast of the Iberian Peninsula. *Continental Shelf Research*, 31: 388–399.
- Alvarez, I., Gomez-Gesteira, M., deCastro, M., and Novoa, E. M. 2008b. Ekman transport along the Galician Coast (NW, Spain) calculated from QuikSCAT winds. *Journal of Marine Systems*, 72: 101–115.
- Alvarez, I., Ospina-Alvarez, N., Pazos, Y., deCastro, M., Bernardez, P., Campor, M. J., Gomez-Gesteira, J. L., *et al.* 2009. A winter upwelling event in the northern Galician Rias: frequency and oceanographic implications. *Estuarine, Coastal and Shelf Science*, 82: 573–582.
- Ambar, I. J., Fiua, A. F. G., Boyd, T., and Frouin, R. 1986. Observations of a warm oceanic current flowing northwards along the coasts of Portugal and Spain during Nov–Dec 1983. *EOS Transactions of the American Geophysical Union*, 67: 1054.
- Bakun, A. 1973. Coastal upwelling indices, west coast of North America, 1946–71. NOAA Technical Report, NMFS 671. 103 pp.
- Bakun, A. 1990. Global climate change and intensification of coastal ocean upwelling. *Science*, 247: 198–201.
- Bode, A., Alvarez-Ossorio, M. T., Cabanas, J. M., Miranda, A., and Varela, M. 2009. Recent trends in plankton and upwelling intensity off Galicia (NW Spain). *Progress in Oceanography*, 83: 342–350.
- Bode, A., Varela, M., Casas, B., and Gonzalez, N. 2002. Intrusions of eastern North Atlantic central waters and phytoplankton in the north and northwestern Iberian shelf during spring. *Journal of Marine Systems*, 36: 197–218.

- Borges, M. F., Santos, A. M. P., Crato, N., Mendes, H., and Mota, B. 2003. Sardine regime shifts off Portugal: a time series analysis of catches and wind conditions. *Scientia Marina*, 67: 235–244.
- Borja, A., Fontan, A., Saenz, J., and Valencia, V. 2008. Climate, oceanography and recruitment: the case of the Bay of Biscay anchovy (*Engraulis encrasicolus*). *Fisheries Oceanography*, 17: 477–493.
- Botas, J., Fernandez, E., Bode, A., and Anadon, R. 1990. A persistent upwelling off the central Cantabrian coast (Bay of Biscay). *Estuarine, Coastal and Shelf Science*, 30: 185–199.
- Casas, B., Varela, M., Canle, M., González, N., and Bode, A. 1997. Seasonal variations of nutrients, seston and phytoplankton, and upwelling intensity off La Coruña (NW Spain). *Estuarine, Coastal and Shelf Science*, 44: 767–778.
- Castro, C. G., Perez, F. F., Alvarez-Salgado, X. A., and Fraga, F. 2000. Coupling between the thermohaline, chemical and biological fields during two contrasting upwelling events off the NW Iberian Peninsula. *Continental Shelf Research*, 20: 189–210.
- deCastro, M., Dale, A. W., Gomez-Gesteira, M., Prego, R., and Alvarez, I. 2006. Hydrographic and atmospheric analysis of an autumnal upwelling event in the Ria of Vigo (NW Iberian Peninsula). *Estuarine, Coastal and Shelf Science*, 68: 529–537.
- deCastro, M., Gomez-Gesteira, M., Alvarez, I., Cabanas, J. M., and Prego, R. 2008. Characterization of fall–winter upwelling recurrence along the Galician western coast (NW Spain) from 2000 to 2005: dependence on atmospheric forcing. *Journal of Marine Systems*, 72: 145–148.
- deCastro, M., Gomez-Gesteira, M., Alvarez, I., and Crespo, A. J. C. 2011. Atmospheric modes influence on Iberian Poleward Current variability. *Continental Shelf Research*, 31: 425–432.
- deCastro, M., Gomez-Gesteira, M., Lorenzo, M. N., Alvarez, I., and Crespo, A. J. C. 2009. Influence on atmospheric modes on coastal upwelling along the western coast of the Iberian Peninsula, 1985 to 2005. *Climate Research*, 36: 169–179.
- desChamps, P. Y., Frouin, R., and Crepon, M. 1984. Sea surface temperatures of the coastal zones of France observed by the HCMM satellite. *Journal of Geophysical Research*, 89: 8123–8149.
- Fernandez, E., and Bode, A. 1991. Seasonal patterns of primary production in the central Cantabrian Sea (Bay of Biscay). *Scientia Marina*, 55: 629–636.
- Fiúza, A. F. G. 1983. Upwelling patterns off Portugal. In *Coastal Upwelling: Its Sediment Record*, Part A, pp. 85–97. Ed. by E. Suess, and J. Thiede. Plenum Press, New York.
- Fiúza, A. F. G. 1984. Hidrologia e dinamica das aguas costeiras de Portugal (Hydrology and dynamics of the Portuguese coastal water). PhD thesis, University of Lisbon. 294 pp.
- Fontan, A., Valencia, V., Borja, A., and Goikoetxea, N. 2008. Oceano-meteorological conditions and coupling in the south-eastern Bay of Biscay, for the period 2001–2005: a comparison with the past two decades. *Journal of Marine Systems*, 72: 167–177.
- Fraga, F. 1981. Upwelling off the Galician Coast, Northwest Spain. In *Coastal Upwelling*, pp. 176–182. Ed. by F. A. Richardson. American Geophysical Union, Washington, DC.
- Frouin, R., Fiúza, A. F. G., Ambar, I., and Boyd, T. J. 1990. Observations of a poleward surface current off the coasts of Portugal and Spain during winter. *Journal of Geophysical Research*, 95: 679–691.
- Garcia-Soto, C., Pingree, R. D., and Valdes, L. 2002. Navidad development in the southern Bay of Biscay: climate change and swoddy structure from remote sensing and *in situ* measurements. *Journal of Geophysical Research*, 107: 3118.
- Gomez-Gesteira, M., deCastro, M., Alvarez, I., and Gomez-Gesteira, J. L. 2008. Coastal sea surface temperature warming trend along the continental part of the Atlantic Arc (1985–2005). *Journal of Geophysical Research*, 113: C04010.
- Gomez-Gesteira, M., Moreira, C., Alvarez, I., and deCastro, M. 2006. Ekman transport along the Galician coast (NW, Spain) calculated from forecasted winds. *Journal of Geophysical Research*, 111: C10005.
- Haynes, R., and Barton, E. D. 1990. A poleward flow along the Atlantic coast of the Iberian Peninsula. *Journal of Geophysical Research*, 95: 11425–11441.
- Koutsikopoulos, C., and Le Cann, B. 1996. Physical processes and hydrological structures related to the Bay of Biscay anchovy. *Scientia Marina*, 60: 9–19.
- Levitus, S., Antonov, J. I., Timothy, P. B., and Stephens, C. 2000. Warming of the world ocean. *Science*, 287: 2225–2229.
- Llope, M., Anadon, R., Viesca, L., Quevedo, M., Gonzalez-Quiros, R., and Stenseth, N. Ch. 2006. Hydrography of the southern Bay of Biscay shelf-break region: integrating the multiscale physical variability over the period 1993–2003. *Journal of Geophysical Research*, 111: C09021.
- Nykjaer, L., and Van Camp, L. 1994. Seasonal and interannual variability of coastal upwelling along northwest Africa and Portugal from 1981 to 1991. *Journal of Geophysical Research*, 99: 14197–14207.
- Otero, J., Alvarez-Salgado, X. A., Gonzalez, A. F., Miranda, A., Groom, S. B., Cabanas, J. M., Casas, G., et al. 2008. Bottom-up control of common octopus *Octopus vulgaris* in the Galician upwelling system, Northeast Atlantic Ocean. *Marine Ecology Progress Series*, 362: 181–192.
- Penabad, E., Alvarez, I., Balseiro, C. F., deCastro, M., Gomez, B., Perez-Muñozuri, V., and Gomez-Gesteira, M. 2008. Comparative analysis between operational weather prediction models and QuikSCAT wind data near the Galician coast. *Journal of Marine Systems*, 72: 256–270.
- Pingree, R. D., and Le Cann, B. 1989. Celtic and Armorican slope and shelf residual currents. *Progress in Oceanography*, 23: 303–338.
- Prego, R., Guzman-Zuñiga, D., Varela, M., deCastro, M., and Gomez-Gesteira, M. 2007. Consequences of winter upwelling events on biogeochemical and phytoplankton patterns in a western Galician Ria (NW Iberian Peninsula). *Estuarine, Coastal and Shelf Science*, 73: 409–422.
- Prego, R., and Vergara, J. 1998. Nutrient fluxes to the Bay of Biscay from Cantabrian rivers (Spain). *Oceanologica Acta*, 21: 271–278.
- Richardson, A. J. 2008. In hot water: zooplankton and climate change. *ICES Journal of Marine Science*, 65: 279–295.
- Richardson, A. J., and Schoeman, D. S. 2004. Climate impact on plankton ecosystems in the Northeast Atlantic. *Science*, 305: 1609–1612.
- Rios, A. F., Perez, F. F., Alvarez-Salgado, X. A., and Figueiras, F. G. 1992. Water masses in the upper and middle North Atlantic Ocean east of the Azores. *Deep Sea Research*, 39: 645–658.
- Santos, A. M., Borges, M. F., and Groom, S. 2001. Sardine and horse mackerel recruitment and upwelling off Portugal. *ICES Journal of Marine Science*, 58: 589–596.
- Tenore, K. R., Alonso-Noval, M., Alvarez-Ossorio, M., Atkinson, L. P., Cabanas, J. M., Cal, R. M., Campos, H. J., et al. 1995. Fisheries and oceanography off Galicia, NW Spain (FOG): mesoscale spatial and temporal changes in physical processes and resultant patterns of biological productivity. *Journal of Geophysical Research*, 100: 10943–10966.
- Torres, R., Barton, E. D., Miller, P., and Fanjul, E. 2003. Spatial patterns of wind and sea surface temperature in the Galician upwelling region. *Journal of Geophysical Research*, 108: 3130–3143.
- Varela, M., Alvarez-Ossorio, M., Bode, A., Prego, R., Bernardez, P., and Garcia-Soto, C. 2010. The effects of a winter upwelling on biogeochemical and planktonic components in an area close to the Galician upwelling core: the Sound of Corcubion (NW Spain). *Journal of Sea Research*, 64: 260–272.
- Varela, M., Prego, R., and Pazos, Y. 2008. Spatial and temporal variability of phytoplankton biomass, primary production and community structure in the Pontevedra Ria (NW Iberian Peninsula):

- oceanographic periods and possible response to environmental changes. *Marine Biology*, 154: 483–499.
- Varela, M., Prego, R., Pazos, Y., and Moroño, A. 2005. Influence of upwelling and river runoff interaction on phytoplankton assemblages in a middle Galician Ria and comparison with northern and southern Rias (NW Iberian Peninsula). *Estuarine, Coastal and Shelf Science*, 64: 721–737.
- Wang, J., Qi, Y., and Jones, I. S. F. 2006. An analysis of the characteristics of chlorophyll in the Sulu Sea. *Journal of Marine Systems*, 59: 111–119.
- Wooster, W. S., Bakun, A., and McClain, D. R. 1976. The seasonal upwelling cycle along the eastern boundary of the North Atlantic. *Journal of Marine Research*, 34: 131–141.

Handling editor: Bill Turrell